Structural Characterization of Residual Soil and the Effect of Drying and Wetting Cycles on Its Strength

Wei Bai[1](✉), Lingwei Kong[1], Liming Xu[2], Xianwei Zhang[1], Zhiliang Sun[1], Ran An[1,3], and Xiu Yue[1,3]

[1] State Key Laboratory of Geomechanics and Geotechnical Engineering, Institute of Rock and Soil Mechanics, Chinese Academy of Sciences, Wuhan, Hubei, China
william_bai@yeah.net

[2] Xiamen Rail Transit Group Limited Corporation, Xiamen, Fujian, China

[3] University of Chinese Academy of Sciences, Beijing, China

Abstract. A series of indoor tests was performed to obtain the physical and mechanical properties and structural characterization of granite residual soil. Experimental results indicated that clot and flocculation are the primary forms of microstructure, and the residual appearance of the parent rock's crystal pattern is reserved. Structural strength is provided by strong cementation and residual chemical bond force. The clay mineral is mostly kaolin, which exhibits a laminated structure. The grain particle of granite residual soil presents the mixed features of sand and clay. The coefficient of compressibility is mostly distributed with in the range of 0.30–0.35 MPa^{-1}, which is for medium compressible soil. Granite residual soil demonstrates good mechanical performance even under saturation condition. However, strength variability is notable. Drying and wetting cycles reduce the strength of granite residual soil, and strength decreases by approximately 30% after two drying and wetting cycles.

Keywords: Residual soil · Physical properties · Strength · Drying and wetting cycles

1 Introduction

Granite residual soil is formed by the physical and chemical weathering of a rock in a hot and humid environment; such soil overlays its parent rock (Shang et al. 2014, 2013). Granite residual soil exhibits fortissimo structural properties. It generally contains a large amount of coarse sand and gravel. In addition, it demonstrates the characteristics of high void ratio, high liquid limit, high strength, and low to medium compressibility. Given the lack of understanding of the characteristics of granite residual soil, several engineering accidents, such as subgrade slope instability and pile foundation failure (Cheng 2002; Liu 1999; Zou and Li 2002), can occur. The distribution area of granite eluvial deposits accounts for approximately 2/3 of the land area of Xiamen (Wang et al. 1990; and Chen and Gong 2014), China. Granite weathered strata, with a thickness of 10–50 m, are

Y. Liu et al. (Eds.): GeoChina 2021, SUCI, pp. 97–111, 2021.
https://doi.org/10.1007/978-3-030-80316-2_10

widely distributed along the metro lines of Xiamen. They compose the major rock and soil layer involved in the construction of foundation pits and other engineering structures. The evident seasonal drying and wetting cycles and the frequent fluctuations of ground water level exert considerable impact on the strength of the granite residual soil in this area. Hence, the acquisition and evaluation of the engineering geological characteristics, material composition, microstructure, and physical and mechanical properties of granite residual soil are highly significant in engineering to avoid accidents and fully utilize the bearing potential of this type of soil.

Therefore, the mineral composition, microstructure characteristics, diameter, grading distribution, drying and wetting cycle effect, and strength parameters of Xiamen granite residual soil were tried and tested in the current study. The engineering geological characteristics of this soil type were also analyzed and evaluated accordingly to provide references for engineering constructions and geological explorations in this area.

2 Engineering Geological Characteristics

Samples were collected from three sites along the Xiamen metro lines located near Xingjin Station (XJ), Lvcuo Station (LC), and Yuanboyuan Station (YB). Through the combination of drilling, standard penetration test (SPT), and field investigation, the soil layer distribution in XJ was determined as follows: ① 0–3.2 m, mixture of clay and gravel; ② 3.2–7.2 m, plastic residual sandy clay with mixed colors of gray–white and yellow–brown, quartz particles smaller than 3 mm in diameter; ③ 7.2–23.0 m, hard plastic residual sandy clay with mixed colors of gray–white and yellow–brown, the content and size of quartz particles increase with depth; ④ 23–27.2 m, completely weathered granite residual soil with yellow–brown color and hard texture, quartz particles are cemented; ⑤ 27.2–30.5 m, moderately to strongly weathered granite residual soil, quartz particle content is smaller compared with that in the upper layer. The soil layer distributions of LC and YB are similar to that of XJ. The relationship between depth and SPT in the three sites is illustrated in Fig. 1. The standard penetration number, $N_{63.5}$, gradually increases with an increase in depth. The physical state changes from plastic to slightly plastic to nonplastic. The strength and foundation bearing capacity gradually increase. A typical distribution pattern of granite strata is presented: the weathering and clayization degree of granite gradually weaken from the shallow portion to the deep region.

Open-pit exploration was performed, and cubic soil samples with dimensions of 25 cm × 25 cm × 25 cm were manually collected from 6 m to 7 m below the surface of the three sites, as shown in Fig. 2(a). No groundwater was found during the process. The samples were packed to make them shock resistant and easy to transport, as shown in Fig. 2(b).

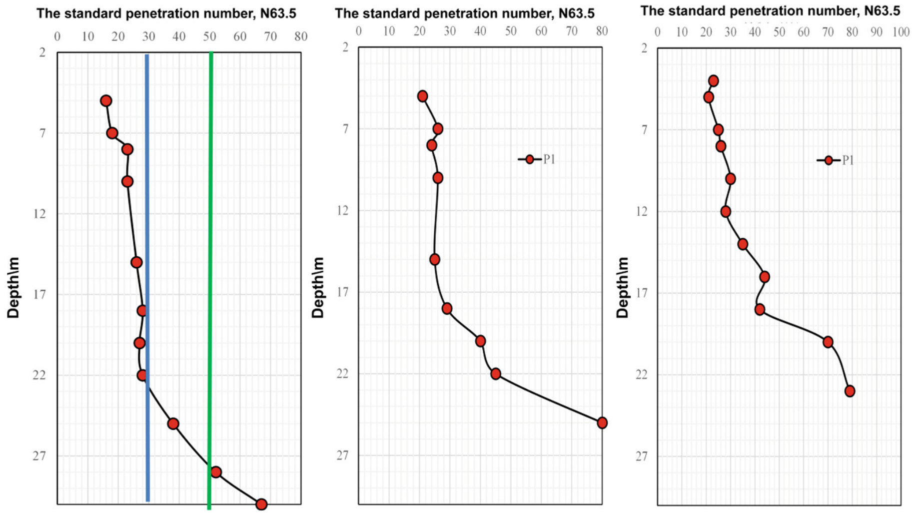

(a) XJ (b) LC (c) YB

Fig. 1. Relationship between depth and SPT

(a) Take undisturbed sample from the test pit (b) Packed the undisturbed samples

Fig. 2. Process of taking the undisturbed sample

3 Composition

Undisturbed soil was ground and passed through a 200-mesh sieve. Mineral composition was analyzed via X-ray diffraction, as shown in Fig. 3. The proportions of kaolin, illite, and quartz in XJ are 37.42%, 9.2%, and 53.38% respectively. The proportions of kaolin and quartz in LC are 24.69% and 75.31%, respectively. Kaolin and quartz in YB account for 33.03% and 66.97%, respectively. The proportion of quartz in Xiamen granite residual soil is the highest, and kaolin is the major clay mineral.

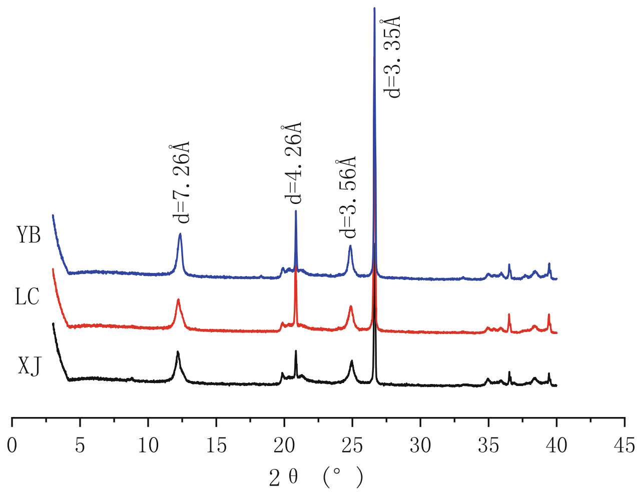

Fig. 3. X-ray diffraction patterns of granite residual soils

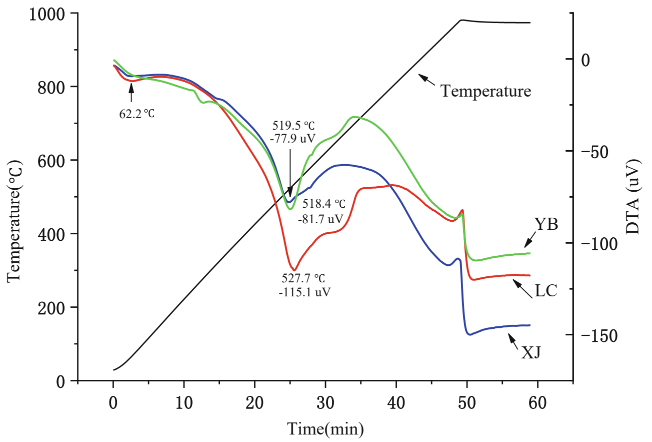

Fig. 4. DTA curves of granite residual soils

The heat absorption valley and exothermic peak in the differential thermal analysis (DTA) curves are caused by the thermal effects of dehydration and phase change during heating. They are related to the composition and structure of granite residual soil. The DTA curves of granite residual soil in XJ, LC, and YB are shown in Fig. 4.

During the temperature increase period of the aforementioned granite residual soil, a small endothermic reaction valley appeared in the DTA curves when temperature reached approximately 62.2 °C. This valley represents the loss of adsorbed water on the particle surface. When the temperature reached approximately 520 °C, the DTA curves presented a large endothermic reaction valley, indicating that a huge amount of adsorbed water escaped within this temperature range and the crystal structure was destroyed during this period. To a certain extent, this endothermic reaction valley can be used to reflect the water absorption capacity of the soil. In general, granite residual soil with a large endothermic reaction valley has high moisture content and viscosity (Zhang 1989). By comparing the DTA curves of the three sites, the endothermic reaction valley of the LC soil sample was found to be the widest. Therefore, the clay particle content of this soil sample is relatively high. The preceding conclusions can be verified in the subsequent study on diameter and grading distribution.

4 Structural Characterization

As shown in Fig. 5, quartz particles are wrapped with clay in the soil samples collected from the three sites. The scanning electron microscopy (SEM) image magnified 100× clearly shows that the quartz particles are lumpy and surrounded by oxides or other cementitious materials in clay Fig. 6(a).

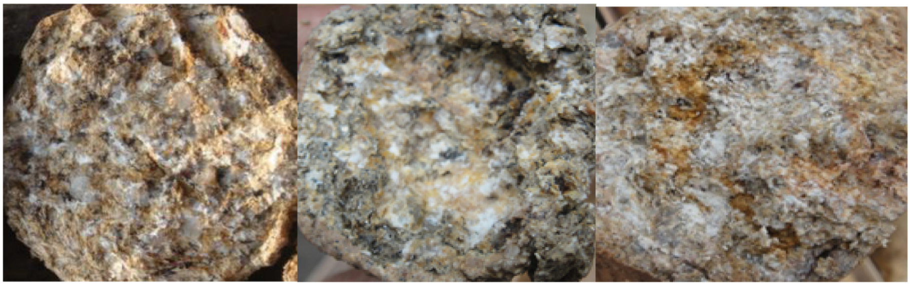

（a）XJ （b）LC （c）YB

Fig. 5. Digital photographs of granite residual soils

When zoomed in to 800× times, the contact mode between particles is found to be dominated by edge-to-face or face-to-face mosaic contact, and the cracks are clear Fig. 6(b). The structure of clay minerals between quartz particles is nondirectional stacking, as shown in Fig. 6(c). This type of structure is attributed to the parent rock gradually weathering into kaolin in an acidic environment. It retains the internal structure characteristics of the primary minerals and the residual chemical bond strength between the grains of the primary minerals. The latter is one of the important reasons for the high mechanical strength of this type of structure. When the clay minerals are enlarged 2000×, the accumulation place of kaolin mineral particles was found to be flat, as shown in Fig. 6(d). This is a typical laminated domain structure of residual soil dominated by kaolin minerals.

From the discussion in the preceding paragraph, the quartz particles in granite residual soil are wrapped by or filled with cement; thus, cementation occurs between particles. However, tests and theoretical studies on soil structure have focused on arrangement characteristics for a long time, but have disregarded the importance of intergranular connection characteristics (Zhang 1994; Wang et al. 2000; Shang et al. 2004). These cementing materials are generally free oxides (Shang et al. 2013) that are sensitive to

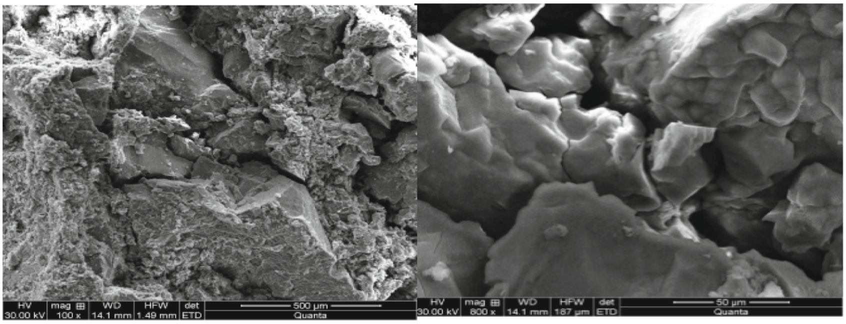

(a) quartz particles at 100× (b) particle contact mode at 800×

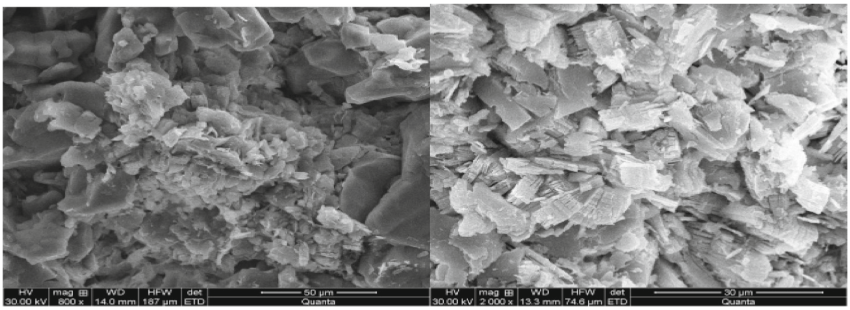

(c) stacking structure of minerals at 800× (d) clay minerals at 2000×

Fig. 6. The SEM photographs of granite residual soils

water content. Mechanical strength easily and abruptly changes under moisture content increase or drying and wetting cycle. Such change is one of the important reasons for the evident structural sensitivity of granite residual soil.

5 Physical Properties

The physical indexes of Xiamen granite residual soil are listed in Table 1. Granite residual soil in the three sites generally have higher natural moisture content and larger void ratio. However, their natural state is basically nonplastic or slightly plastic. The liquid limits of the fine particle group of the three aforementioned granite residual soil samples are all higher than 50%, and their plasticity indexes are all greater than 22. In the plastic index diagram, XJ and YB are located slightly lower than Line A (MH) but LC is located slightly higher than Line A (CH). This finding indicates that the fine particle group of Xiamen granite residual soil exhibits the properties of high liquid limit clay and silty clay.

The particle composition of the granite residual soil mentioned above is special. The quality of particles with a diameter greater than 0.075 mm is not more than 50% of the total quality, and the plasticity index is greater than 17. Thus, such type of soil should be classified as clay on the basis of standards (Ministry of Construction 2009). However,

Table 1. Indexes of physical properties of granite residual soils

Soil sample	XJ	LC	YB
Depth (m)	6.0	6.5	7.0
Average moisture content (%)	23.4	31.0	25.7
Wet density (g/cm^3)	1.84	1.76	1.82
Dry density (g/cm^3)	1.49	1.34	1.45
Liquid limit (%)	58.5	51.8	51.4
Plastic limit (%)	31.4	27.9	28.6
Plasticity index	27.1	23.9	22.8
Specific gravity	2.7	2.7	2.7
Void ratio	0.81	1.01	0.86
Saturation degree (%)	77.9	82.9	80.2
Particle composition (%)			
10~5 mm	14.3	0.4	4.2
5~2 mm	13.8	14.3	20.4
2~0.5 mm	10.7	12.7	12.9
0.5~0.25 mm	4.4	6.2	5.2
0.25~0.075 mm	3.6	7.0	3.0
0.075~0.005 mm	39.3	42.8	29.8
<0.005 mm	13.9	16.6	24.5

the quality of particles with a diameter greater than 2 mm is close to or more than 25% of the total quality. Clay does not reflect such characteristics, and thus, classifying such soil as *residual gravel clay* is more appropriate in reference with the local standards (Fujian Provincial Department of Construction 2006). The proportion of coarse particles and fine particles is large, while the content of particles with intermediate particle size is small. Moreover, the aforementioned characteristics of particle diameter distribution provide possible conditions for small particles to flow out from the pores of large particles. When hydrodynamic pressure is too high, seepage deformation phenomena, such as piping and flowing soil, may easily occur. Therefore, effective water-sealing measures should be implemented in important projects. The data in Table 1 indicate that the proportion of the fine particle group of the LC soil samples reaches as high as 59.4%, exceeding those of the XJ (53.2%) and YB (54.3%) soil samples. This result is consistent with the conclusion that the LC soil samples with the widest endothermic reaction valley have a higher content of viscous particles in the DTA curves. Permeation tests were also conducted on 10 samples from each site. The change range of the XJ soil samples' permeability coefficient is 1.01×10^{-5}–3.90×10^{-4} cm·s^{-1}. The change range of the LC soil samples' permeability coefficient is 7.43×10^{-6}–9.07×10^{-5} cm·s^{-1}. The change range of the YB soil samples' permeability coefficient is 8.11×10^{-6}–$1.66 \times$

10^{-4} cm·s^{-1}. The histogram of the permeability coefficient of the three sites is presented in Fig. 7. The probability that the permeability coefficient of the sample is 10^{-5} cm·s^{-1} is the highest. Therefore, they belong to a weak permeable grade.

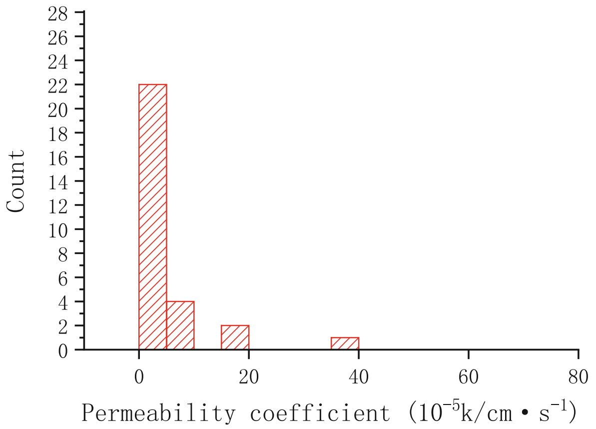

Fig. 7. Histogram of permeability coefficient

6 Mechanical Properties

6.1 Compressibility

Undisturbed soil samples were cut useing a ring knife (61.8 mm in diameter and 20 mm in height). 10 samples were collected from each site for the standard consolidation tests. The histogram of the compressibility coefficient is presented in Fig. 8.

As shown in the figure, the compressibility coefficient (a_{1-2}) of each sample is between 0.15 MPa^{-1} and 0.45 MPa^{-1}. Most of the values are within the range of 0.30–0.35 MPa^{-1} and can be classified as medium compressibility soil. The compressibility of XJ and YB is lower than that of LC.

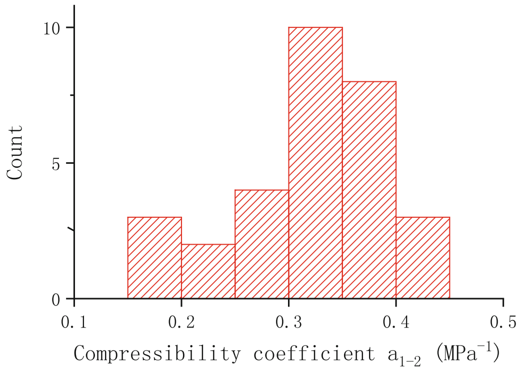

Fig. 8. Histogram of compressibility coefficient

6.2 Consolidated Undrained (CU) Triaxial Tests

Undisturbed soil samples were cut into cylindrical soil samples (diameter: 39.1 mm, height: 80 mm) in accordance with the standard (Ministry ofWater Resources 2019). Triaxial compression tests (CU and consolidated shear tests) were performed after reaching saturation (vacuum pumping saturation method). The shear rate was set as 0.060 mm/min. Nine to ten tests were conducted at each site. The typical failure modes of the soil samples from the three sites after the CU tests are shown in Fig. 9. No obvious shear plane appeared when axial strain reached 20%.

Fig. 9. The failure mode of granite residual soil samples after the CU tests

The CU shear strength indexes (cohesion and internal friction angle) obtained in the preceding tests are provided in Table 2.

Table 2. Consolidated undrained triaxial tests results of granite residual soils

Soil sample	c_{cu}/kPa	φ_{cu}/°	Soil sample	c_{cu}/kPa	φ_{cu}/°	Soil sample	c_{cu}/kPa	φ_{cu}/°
XJ1	33.1	25.1	LC1	64.2	15.3	YB1	22.3	29.9
XJ2	56.5	22.7	LC2	40.7	19.8	YB2	74.7	19.3
XJ3	44.0	23.5	LC3	61.4	13.8	YB3	83.3	15.9
XJ4	54.1	19.8	LC4	–	–	YB4	43.8	19.0
XJ5	–	–	LC5	38.5	18.8	YB5	49.4	22.0
XJ6	41.9	23.1	LC6	60.0	14.0	YB6	24.5	23.6
XJ7	59.5	22.3	LC7	46.6	18.1	YB7	24.5	23.6
XJ8	61.2	22.5	LC8	84.8	13.1	YB8	21.3	30.1
XJ9	55.6	22.6	LC9	58.7	17.3	YB9	74.2	20.1
XJ10	51.7	23.8	LC10	59.2	16.2	YB10	78.4	19.6

The c_{cu} of XJ ranges from 33.1 kPa to 61.2 kPa. Its mean value is 50.8 kPa, its standard deviation is 8.8 kPa, and its variable coefficient is 0.17. The φ_{cu} of XJ ranges from 19.8° to 25.1°. Its mean value is 22.8°, its standard deviation is 1.3°, and its variable coefficient is 0.03. The c_{cu} of LC ranges from 38.5 kPa to 84.8 kPa. Its mean value is 57.1 kPa, its standard deviation is 13.2 kPa, and its variable coefficient is 0.23. The φ_{cu} of LC ranges from 13.1° to 19.8°. Its mean value is 16.3°, its standard deviation is 2.2°, and its variable coefficient is 0.14. The c_{cu} of YB ranges from 21.3 kPa to 83.3 kPa. Its mean value is 49.6 kPa, its standard deviation is 24.6 kPa, and its variable coefficient is 0.50. The φ_{cu} of YB ranges from 13.1° to 19.8°. Its mean value is 16.3°, its standard deviation is 2.2°, and its variable coefficient is 0.14. The data of the strength parameters of the CU and consolidated shear tests indicate that even in a saturated state, the granite residual soil samples exhibit higher cohesion and internal friction angle and still have better mechanical properties. However, although the three sites are basically located in the same soil layer, the quality of the soil samples is not uniform, presenting a highly variable coefficient of cohesion. Xiamen residual soil is the debris formed by the weathering of a rock. Thus, variation in mechanical parameters will be caused by different forms of primary and secondary structural surfaces, particle size distribution among soil samples, and connection patterns of wrapping and filling oxide. Therefore, the inhomogeneity of residual soil should be considered fully in practical projects, and parameters should be selected on the basis of in-situ test data as much as possible in major projects.

6.3 Drying and Wetting Cycles

Undisturbed soil samples were cut into cylindrical soil samples (diameter: 39.1 mm, height: 80 mm) in accordance with the standards. The drying and wetting cycle range was between 15% and 30% (saturated moisture content was approximately 30%; it slightly varied for soil samples from different sites). Humidification was performed using the standard method (i.e., vacuum pumping saturation). Dehumidification was conducted via air-drying: the samples were removed from the saturator, placed on a tray, and air-dried to the specified moisture content (monitored by weighing). To ensure the uniformity of moisture concent in the soil sample after air drying, the soil sample must be sealed with plastic film and then placed in a moisturizing tank for 24 h. The specific process of the drying and wetting cycle tests is illustrated in Fig. 10. Four sets of samples were prepared for each site, for a total of twelve sets of samples. The unconfined compressive strength indexes were obtained using a YYW-2 unconfined compression tester.

The test results of the samples from the three sites were analyzed. The decay rate is defined as the ratio of the difference of the unconfined compressive strength between samples of n cycles and samples of 0 cycles to the strength corresponding to 0 cycles, as shown in Eq. (1).

$$\Delta = \left| \frac{q_{un} - q_{u0}}{q_{u0}} \right| \times 100\% \tag{1}$$

Where, q_{un} is the unconfined compressive strength of the soil samples that have undergone n-th drying and wetting cycles, and q_{u0} is the unconfined compressive strength of the soil samples that have not undergone a drying and wetting cycle.

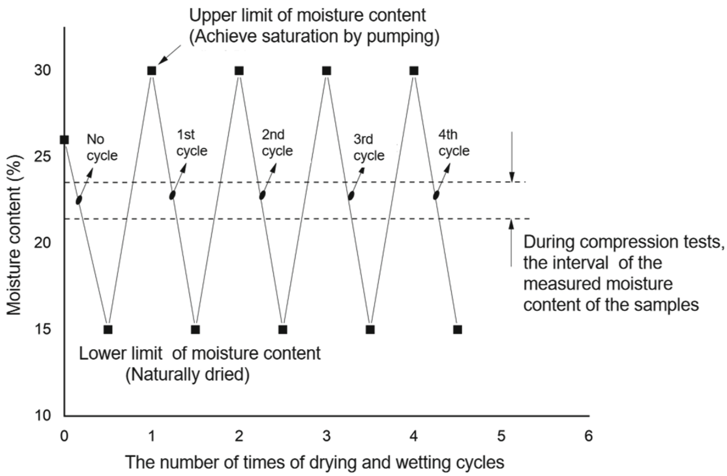

Fig. 10. The sketch of the drying and wetting cycle

The relationship among unconfined compressive strength, decay, and drying and wetting cycles is shown in Fig. 11. The statistical test results are provided in Table 3.

As indicated in Fig. 11 and Table 3, unconfined compressive strength decreases rapidly after a drying and wetting cycle. The attenuation amplitude of the XJ soil sample is the largest (30.6%), followed by that of the YB soil sample (22.1%) and then the LC soil sample (19.1%). After a second drying and wetting cycle, the attenuation amplitude of the XJ and YB soil samples is approximately 10%, except for the large reduction (46.2%) in LC. The change amplitude of all the soil samples in the third and fourth cycles is less than 4%. Therefore, a conclusion can be drawn that the drying and wetting cycle considerably influences the unconfined compressive strength of granite weathered soil samples. In addition, the unconfined compressive strength tends to become stable after two drying and wetting cycles.

Xiamen granite residual soil is mostly composed of residual clastic materials formed in situ after the weathering of a rock mass. Most of the rock is completely weathered into mineral particles. The common feature of residual soil and weathered rocks, except for isolated rocks, is that they remained in the location of the original rock without being transported and sorted by other media. There must be primary and secondary structural planes in the residual soils, and the structure of the original rock is relatively preserved between the mineral particles. The drying and wetting cycle affects the structure of residual soil, generating more microcracks and reducing the strength of soil. Moreover, the properties of cementing materials irreversibly weaken during the drying and wetting cycle, reducing the structural strength of granite residual soil.

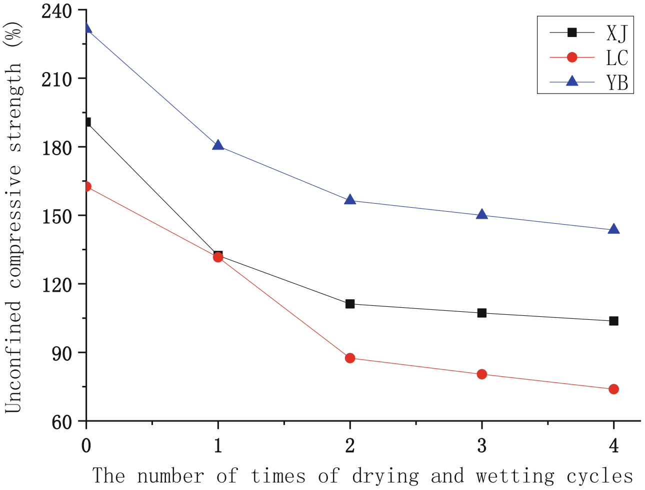

(a) Relationship between unconfined compressive strength and drying and wetting cycles

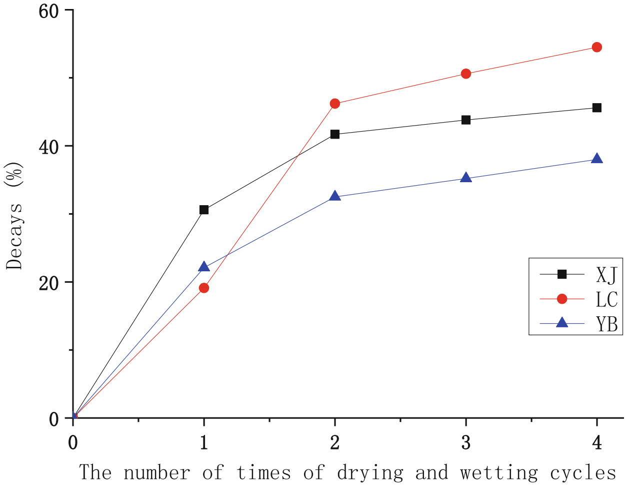

(b) Relationship between decays and drying and wetting cycles

Fig. 11. Relationship between unconfined compressive strength, decays and drying and wetting cycles

Table 3. The unconfined compression tests results after drying and wetting cycles

Soil samples	Number of times of cycles	Unconfined compressive strength (kPa)	Moisture content (%)	Decays (%)
XJ	0	190.8	20.7	0.0
	1	132.4	20.1	30.6
	2	111.2	20.0	41.7
	3	107.2	20.2	43.8
	4	103.7	20.5	45.6
LC	0	162.6	22.1	0.0
	1	131.6	22.0	19.1
	2	87.5	22.5	46.2
	3	80.4	22.3	50.6
	4	73.9	22.6	54.5
YB	0	231.5	20.8	0.0
	1	180.3	20.5	22.1
	2	156.4	20.9	32.5
	3	150.0	20.1	35.2
	4	143.6	22.6	38.0

7 Conclusions

A series of tests were applied to determine the physical, mechanical and structural characteristics of the typical granite residual soil in Xiamen, China, namely, drilling, standard penetration tests (SPT), open-pit exploration, X-ray diffraction, differential thermal analyses (DTA), scanning electron microscopy (SEM), liquid limit and plastic limit tests, particle diameter analyses, permeability tests, standard consolidation tests, consolidated undrained (CU) triaxial tests and drying-wetting cycle tests. On the basis of the obtained results, the following conclusions can be drawn:

(1) The special properties of Xiamen granite residual soil are closely related to its composition and structure. Its structural characterization retains the residual form of the crystal structure of its parent rock, primarily in the form of clot and flocculation. Structural strength mostly originates from the strong cementing force of oxide and the remaining chemical bonding force. Quartz particles are wrapped by or filled with cement. The edge-to-surface or surface-to-surface inlay contact is the major contact mode between particles. The composition of clay minerals is largely kaolin, which exhibits a typical laminated domain structure.
(2) The particle composition of Xiamen granite eluvial soil is special. It presents the characteristics of sand, gravel, and clay. The characteristics of particle diameter distribution provide possible conditions for small particles to flow out from the

pores of large particles. For important projects, such as foundation pits, effective water-sealing measures should be implemented to avoid seepage deformation, such as piping and flowing soil.

(3) The coefficient of compressibility of granite residual soil from the three sites in Xiamen is mostly distributed within the range of 0.30–0.35 MPa^{-1}, which is for medium compressible soil. The compressibility of XJ and YB is lower than that of LC. The CU shear tests show that Xiamen granite residual soil exhibits better mechanical performance even under saturated condition. However, strength variability is notable, and nonuniformity should be considered fully in practical engineering.

(4) The drying and wetting cycle affects the structure of granite residual soil. It generates more microcracks and irreversibly weakens the properties of the cementing materials and structural connections, leading to the strength attenuation of the granite residual soil. After two drying and wetting cycles, the decay rate of unconfined compressive strength is over 30%. Thereafter, the influence of increasing the number of drying and wetting cycles on unconfined compressive strength is decreased.

(5) The above conclusions can provide valuable references for engineering construction and engineering geological exploration, and are of great engineering significance for avoiding accidents and making full use of the bearing potential of granite residual soil.

Acknowledgments. The project are funded by the National Natural Science Foundation of China (Grant No. 41772339).

References

Cheng, J.: The failure reasons of manually excavated pile in the residual area. Geotech. Eng. World (02), 36–37 (2002)

Chen, D., Gong, X.: Experiment and modeling of soil-water characteristic curve of unsaturated residual soil. Rock Soil Mech. **35**(07), 1885–1891 (2014)

Fujian Provincial Department of Construction: Local standards for engineering construction in Fujian Province: code for investigation of geotechnical engineering (2006)

Liu, D.: The failure case study of hand-dug pile foundation in Xiamen. Geotech. Eng. Tech. (04), 59–62 (1999)

Ministry of Construction, PRC: Code for Investigation of Geotechnical Engineering. China Construction Industry Press, Beijing (2009)

Ministry of Water Resources, PRC: Standard for geotechnical testing method, China (2019)

Shang, L., Sang, H., Hou, T., et al.: Experimental study on tensile strength of granite residual soil. ACTA Scientiarum Naturalium Univ. Sunyatseni **53**(06), 98–105 (2014)

Shang, L., Sang, H., Song, J., et al.: Research on soil particle joint function and brittle-elastoplastic cement damage model of unsaturated granite residual soil. Rock Soil Mech. **34**(10), 2877–2888 (2013)

Shang, Y., Wang, S., Yue, Z., et al.: Variation features of pore radius and particle diameter distributions and mineral content of completely decomposed granite and correlation of parameters. Rock Soil Mech. **25**(10), 1545–1550 (2004)

Wang, Q., Jiang, H., Tang, D.: A study on engineering geological properties of granitic residual soil in south Fujian. Geol. Fujian **9**(02), 90–99 (1990)
Wang, Y., Xie, X., Wang, C.: Physical properties of the profiles of weathered granitic rocks in Guangdong. Trop. Geogr. (04), 256–260 (2000)
Zou, J., Li, Z.: Research on the stability of completely decomposed granite cut slope. Hunan Commun. Sci. Technol. (01), 25–26+38 (2002)
Zhang, Q.: A study on the relationship between DTA curves and physico-chemical properties of bentonite. ACTA Mineral. Sin. (02), 177–180 (1989)
Zhang, W.: Analysis of the shear strenth of granitic residual soil and the destablization of soil slope. Hydrogeol. Eng. Geol. (03), 41–43 (1994)